

Effect of Sb composition on the band alignment of InAs/GaAsSb quantum dots

Guangze Lu(陆光泽), Zunren Lv(吕尊仁), Zhongkai Zhang(张中恺), Xiaoguang Yang(杨晓光), and Tao Yang(杨涛)
Citation: Chin. Phys. B, 2021, 30 (**1**): 017802. DOI: 10.1088/1674-1056/abb309
Journal homepage: http://cpb.iphy.ac.cn; http://iopscience.iop.org/cpb

What follows is a list of articles you may be interested in

Optical properties of core/shell spherical quantum dots

Shuo Li(李硕), Lei Shi(石磊), Zu-Wei Yan(闫祖威)
Chin. Phys. B, 2020, 29 (**9**): 097802. DOI: 10.1088/1674-1056/ab961a

Monolithic semi-polar (1101) InGaN/GaN near white light-emitting diodes on micro-striped Si (100) substrate

Qi Wang(王琦), Guo-Dong Yuan(袁国栋), Wen-Qiang Liu(刘文强), Shuai Zhao(赵帅), Lu Zhang(张璐), Zhi-Qiang Liu(刘志强), Jun-Xi Wang(王军喜), Jin-Min Li(李晋闽)
Chin. Phys. B, 2019, 28 (**8**): 087802. DOI: 10.1088/1674-1056/28/8/087802

Large-scale control of enhancement and quenching of photoluminescence for ZnSe/ZnS quantum dots and Ag nanoparticles in aqueous solution

Shaoyi Yin(殷少轶), Liming Liao(廖李明), Song Luo(罗松), Zhe Zhang(张喆), Xiaoyu Zhang(张晓宇), Jian Lu(鹿建), Zhanghai Chen(陈张海)
Chin. Phys. B, 2019, 28 (**5**): 057803. DOI: 10.1088/1674-1056/28/5/057803

Preparation and photoelectric properties of cadmium sulfide quantum dots

Yue Gu(古月), Libin Tang(唐利斌), Xiaopeng Guo(郭小鹏), Jinzhong Xiang(项金钟), Kar Seng Teng, Shu Ping Lau(刘树平)
Chin. Phys. B, 2019, 28 (**4**): 047803. DOI: 10.1088/1674-1056/28/4/047803

SnS_2 quantum dots: Facile synthesis, properties, and applications in ultraviolet photodetector

Yao Li(李尧), Libin Tang(唐利斌), Rujie Li(李汝劼), Jinzhong Xiang(项金钟), Kar Seng Teng, Shu Ping Lau(刘树平)
Chin. Phys. B, 2019, 28 (**3**): 037801. DOI: 10.1088/1674-1056/28/3/037801

Effect of Sb composition on the band alignment of InAs/GaAsSb quantum dots*

Guangze Lu(陆光泽)[1,2], Zunren Lv(吕尊仁)[1], Zhongkai Zhang(张中恺)[1,2], Xiaoguang Yang(杨晓光)[1,2,†], and Tao Yang(杨涛)[1,2]

[1] *Key Laboratory of Semiconductor Materials Science, Institute of Semiconductors, Chinese Academy of Sciences, Beijing* 100083, *China*
[2] *Center of Materials Science and Optoelectronics Engineering, University of Chinese Academy of Sciences, Beijing* 100049, *China*

(Received 28 June 2020; revised manuscript received 19 August 2020; accepted manuscript online 27 August 2020)

Aiming to achieve InAs quantum dots (QDs) with a long carrier lifetime, the effects of Sb component in cap layers on the band alignment of the InAs/GaAsSb QDs have been studied. InAs QDs with high density and uniformity have been grown by molecular beam epitaxy. With increasing Sb composition, the InAs/GaAsSb QDs exhibit a significant red-shift and broadening photoluminescence (PL). With a high Sb component of 22%, the longest wavelength emission of the InAs/$GaAs_{0.78}Sb_{0.22}$ QDs occurs at 1.5 μm at room temperature. The power-dependence PL measurements indicate that with a low Sb component of 14%, the InAs/$GaAs_{0.86}Sb_{0.14}$ QDs have a type-I and a type-II carrier recombination processes, respectively. With a high Sb component of 22%, the InAs/$GaAs_{0.78}Sb_{0.22}$ QDs have a pure type-II band alignment, with three type-II carrier recombination processes. Extracted from time-resolved PL decay traces, the carrier lifetime of the InAs/$GaAs_{0.78}Sb_{0.22}$ QDs reaches 16.86 ns, which is much longer than that of the InAs/$GaAs_{0.86}Sb_{0.14}$ QDs (2.07 ns). These results obtained here are meaningful to realize high conversion efficiency intermediate-band QD solar cells and other opto-electronic device.

Keywords: quantum dots, type-II band alignment, intermediate-band solar cell, molecular beam epitaxy

PACS: 78.67.Hc, 78.66.Fd, 78.67.–n **DOI:** 10.1088/1674-1056/abb309

1. Introduction

As zero-dimension active gain materials, quantum dots (QDs) have been widely used in opto-electronic devices, such as communication lasers,[1,2] silicon photonics transmitters,[3] infrared detectors,[4,5] Q-bit emitters,[6] and intermediate-band solar cells (IBSC).[7,8] To enhance the performance of IBSCs and infrared detectors, QDs with long carrier lifetime are highly desirable.[9] During last decade, InAs/GaAsSb QDs have attracted much interest because of its variable band alignment. A rapid decrease in the valence-band energy of GaAsSb cap layer with increasing Sb composition result in a type-II band alignment.[10] The spatial separation of electron–hole pairs in InAs/GaAsSb QDs with a type-II band alignment is expected to lead to reduced carrier recombination and increased carrier lifetime. Recently, some groups have reported IBSCs based on InAs/GaAsSb QDs with a type-II band alignment.[11,12] Contrary to theoretical expectations, all these devices show dropped open-circuit voltages and efficiencies compared with reference IBSCs based on InAs/GaAs QDs with a type-I band alignment. One of the reasons is the low carrier lifetime of the fabricated InAs/GaAsSb QDs. As reported so far, the carrier lifetime of InAs/GaAsSb QDs with a type-II band alignment are generally a few nanoseconds.[13,14] The high density of strain-induced dislocations inside the InAs/GaAsSb QDs caused a minority carrier recombination, leading the open-circuit voltage degradation. Another reason is that the band alignment of InAs/GaAsSb QDs needs to be further revealed. Most studies consider that there is only one carrier recombination process in InAs/GaAsSb QDs, which lead to a much simplified band structure.[15]

In this work, InAs/GaAsSb QDs with different Sb components in the cap layers have been grown using molecular beam epitaxy (MBE). The effect of Sb component on the band alignment and related carrier recombination processes of InAs/GaAsSb QDs have been studied. Photoluminescence (PL) and power-dependent PL measurements have been used to characterize the properties of the InAs/GaAsSb QDs. The results reveal that the band alignment of InAs/GaAsSb QDs is strongly effected by Sb component. When the Sb component is 14%, InAs/$GaAs_{0.86}Sb_{0.14}$ QDs show a complex band structure, with a type-I and a type-II carrier recombination processes respectively. It indicates that the QDs is in the critical state of transformation between type-I and type-II. As the Sb component is increased to 22%, InAs/$GaAs_{0.78}Sb_{0.22}$ QDs exhibit three carrier recombination processes, and all of them are from the type-II band alignments. To obtain further insight into the dynamic mechanism, the time-resolved PL measurements have also been tested. The results show that the

*Project supported by the National Key Research and Development Program of China (Grant Nos. 2019YFB1503601 and 2017YFB0405302), the National Natural Science Foundation of China (Grant Nos. 61574139 and U1738114), and the Strategic Priority Research Program on Space Science, the Chinese Academy of Sciences (Grant No. XDA15051200).

†Corresponding author. E-mail: xgyang@semi.ac.cn

© 2021 Chinese Physical Society and IOP Publishing Ltd

carrier lifetime of InAs/$GaAs_{0.78}Sb_{0.22}$ QDs reaches 16.86 ns, which is about 8-times longer than that of InAs/$GaAs_{0.86}Sb_{0.14}$ QDs (2.07 ns). The remarkably increased carrier lifetime offers a substantial potential for the enhancement of novel optoelectronic applications.

2. Experiment

Samples used in the study were grown using a Riber Compact-21 MBE system. As schematically illustrated in Fig. 1(a), all of samples were grown on n^+-GaAs (100) substrates. After the substrate deoxidation, a 500-nm GaAs buffer layer was first deposited at 580 °C. Then the temperature was cooled down to 470 °C, and an inner layer of InAs QDs was grown with a coverage of 3.0 monolayers. After a 30-second pause, the inner InAs QDs were covered by a 5-nm low-temperature cap layer which was grown at 470 °C. The components of low-temperature cap layers were $In_{0.18}Ga_{0.82}As$ for sample A that was a reference, $GaAs_{0.86}Sb_{0.14}$ for sample B, and $GaAs_{0.78}Sb_{0.22}$ for sample C, respectively. Then the temperature was increased to 600 °C, and a 95-nm high-temperature GaAs cap layer was subsequently grown. Finally, the temperature was cooled down to 470 °C, and surface InAs QDs which were used for atomic force microscopy (AFM) test were grown under the same growth conditions as the inner InAs QDs. Figure 1(b) shows a typical AFM image of the surface InAs QDs. The density of QDs is approximately 6×10^{10} cm^{-2}. It is found that the InAs QDs have a good uniformity, their average height and diameter are 3 nm and 35 nm, respectively.

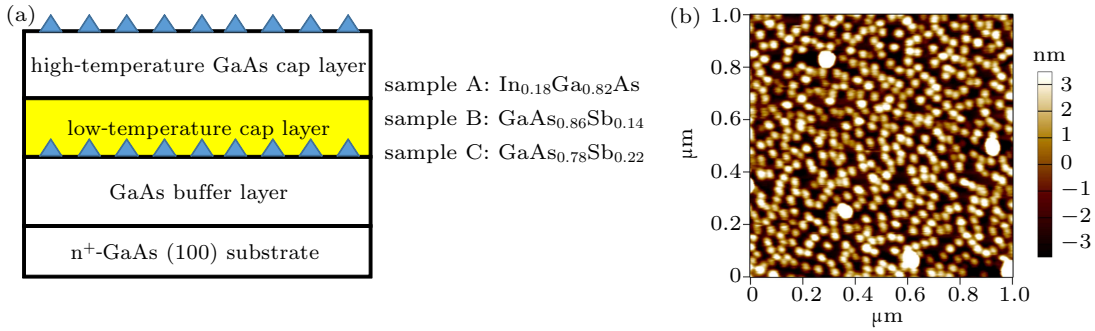


Fig. 1. (a) Schematic structure of samples with different low-temperature cap layers, (b) AFM image of the surface InAs QDs.

3. Results and discussion

Figure 2 shows the PL spectra of samples measured at a low temperature of 12 K and room temperature (RT). At 12 K, sample A exhibits a sharp emission peak at 1215 nm. The full-width at half-maximum (FWHM) of the peak is only 29.5 meV, which implies a quite good uniformity of the InAs QDs. The emission peak of sample B locates at 1188 nm and has an FWHM of about 48 meV. The increased spectral linewidth for sample B could be related to the segregation of Sb atoms in the GaAsSb cap layer. Sample C shows in turn a significant red-shift emission peak at 1280 nm. At RT, the FWHM of emission peak of sample A is still a small value, but the emission peaks of sample B and sample C obviously broaden. Because of the electron thermal excitation, more energy levels in QDs can be filled in at RT, which could cause a wider Gaussian-peak. Furthermore, sample C shows a fairly wide emission peak, with the longest wavelength emission occurring at 1500 nm.

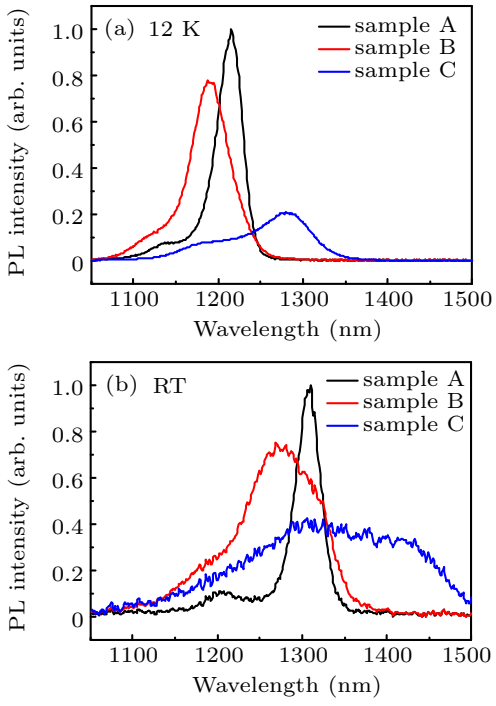


Fig. 2. PL spectra of samples measured at (a) 12 K and (b) RT.

To further investigate the band structures of samples, power-dependent PL measurements were performed at 12 K. The excitation powers were varied from 5 mW to 500 mW. The power-dependent PL spectra of samples as well as their peak energies as a function of excitation powers are shown in Fig. 3. With increasing excitation power, the peak intensity of the peak 1 for sample A rapidly saturates and the peak intensity of the peak 2 correspondingly significantly increases, as shown in Fig. 3(a). Meanwhile, the peak energies of the two peaks for sample A remain unchanged as the excitation power increases. It indicates that the band alignment of InAs/$In_{0.18}Ga_{0.82}As$

quantum dots for sample A is typically type-I. It is found from Fig. 3(b), as the excitation power increases, the peak energy of the peak 1 for sample B is nearly unchanged. However, the peak energy of the peak 2 exhibits a linear increase with the excitation power, which indicates that the carrier recombination processes related to the peak 2 is type-II. Moreover, for sample C, all of the peaks show a significant and linear blue-shift with the excitation power, as shown in Fig. 3(c), which implies a pure type-II band alignment of the InAs/GaAs$_{0.78}$Sb$_{0.22}$ QDs.[16,17]

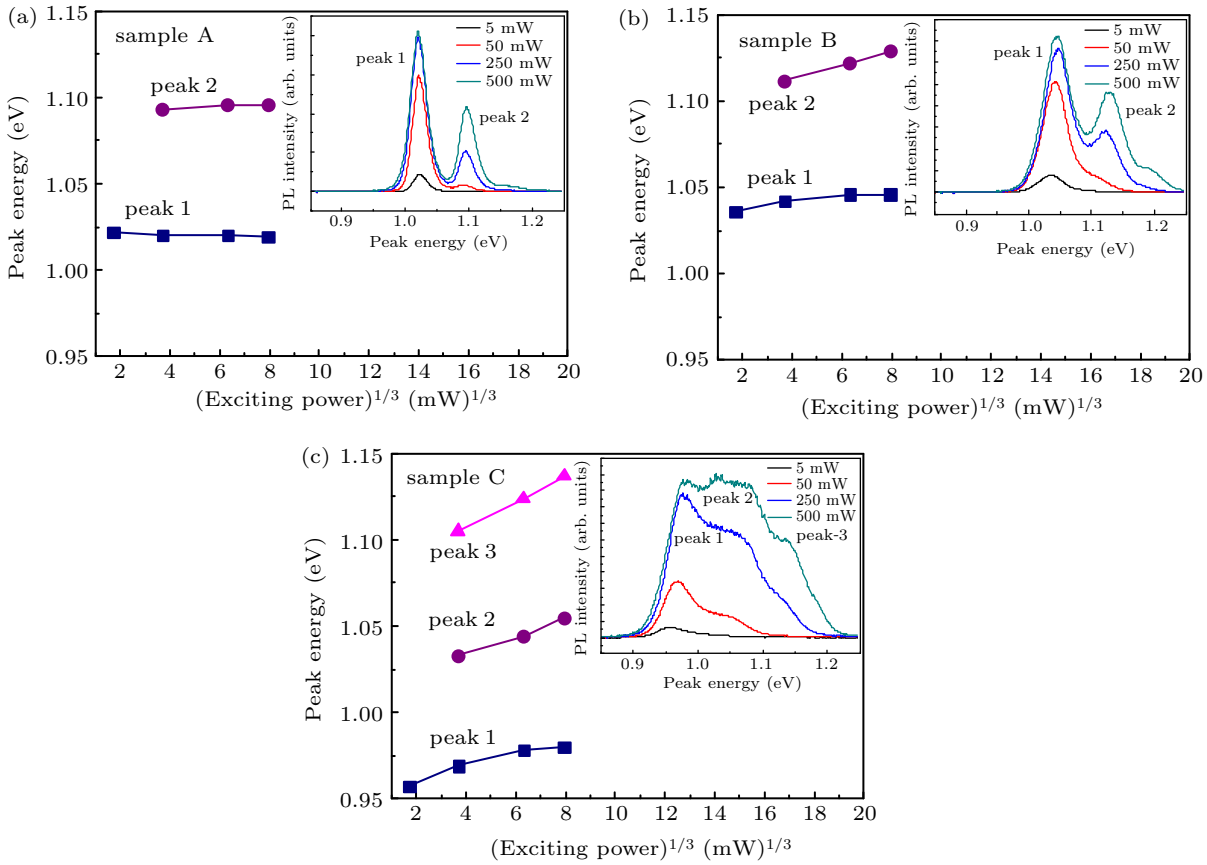


Fig. 3. The peak energies as a function of the excitation powers for samples measured at 12 K. The insets show the power-dependent PL spectra of samples with increased excitation power from 5 mW to 500 mW.

To further confirm the band alignment of samples, time-resolved PL decay traces were measured at 10 K. The test system were performed using a 532-nm semiconductor laser as the excitation source. The signal was collected using a diffraction-limited confocal microscope objective and measured by a time correlated single photon counting (TCSPC) device. Using an exponential function

$$I(t) = A\exp\left(-\frac{t}{\tau}\right) + I_0, \tag{1}$$

the time constant (τ) of the QDs related to each peak for samples was extracted. Figure 4 shows the time-resolved PL decay traces of the emission peaks for samples and their schematic illustrations of the corresponding carrier recombination processes. For the InAs/In$_{0.18}$Ga$_{0.82}$As QDs of sample A, τ related to the peak 1 and peak 2 is 1.02 ns and 0.48 ns, which indicate that the peak 1 and peak 2 resulted from the $(E_0 \rightarrow H_0)$ and $(E_1 \rightarrow H_1)$ transitions, respectively. For the InAs/GaAs$_{0.86}$Sb$_{0.14}$ QDs of sample B, τ related to peak 1 and peak 2 is 1.04 ns and 2.07 ns. Due to strong intermixing between As atoms and Sb atoms, an As–Sb alloy layer will form between InAs QDs and GaAsSb cap layers. When the Sb component is low, the As-Sb alloy layer will localize the holes into the InAs and GaAsSb valence band respectively.[18] Combined with the power-dependent PL measurement, peak 1 and peak 2 were the emission peaks of $(E_0 \rightarrow H_0)$ and $(E_0 \rightarrow H_0')$ transitions. For InAs/GaAs$_{0.78}$Sb$_{0.22}$ QDs of sample C, τ related to three peaks is 5.50 ns, 2.87 ns, and 16.86 ns, respectively. When the Sb component is high, all holes are localized in GaAsSb valence band.[19] Also combined with the power-dependent PL measurement, the peak 1 and peak 2 originate from the $(E_0 \rightarrow H_0)$ and $(E_1 \rightarrow H_1)$ transitions, the peak 3 is resulted from $(E_{\mathrm{GaAs}} \rightarrow H_0)$ transition. Clearly, the spatial separation of the electrons and holes for InAs/GaAsSb QDs with type-II band alignment results in a much longer lifetime. Based on the QDs with long carrier lifetime, a high conversion efficiency of intermediate-band QD solar cells can be expected.

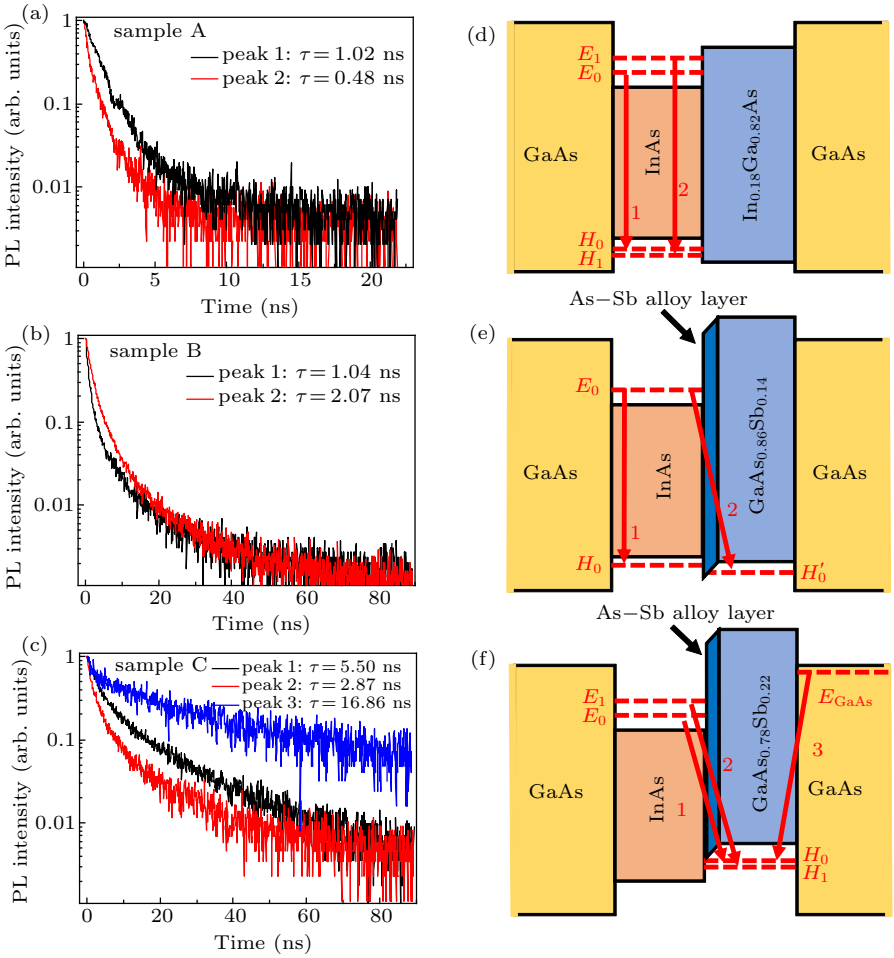


Fig. 4. (a)–(c) Time-resolved PL spectra of simples and the time constant of each peak. (d)–(f) The band structure scheme of simples and the carrier recombination processes related to each peaks.

4. Conclusions

The band structures of InAs/GaAsSb QDs with different Sb component have been comparatively studied by PL, power-dependent PL, and time-resolved PL measurements. InAs/$GaAs_{0.86}Sb_{0.14}$ QDs have a complex band alignment, with type-I and type-II carrier recombination processes. InAs/$GaAs_{0.78}Sb_{0.22}$ QDs have a pure type-II band alignment with three type-II carrier recombination processes. Because the spatial separation of the electrons and holes, InAs/GaAsSb QDs with type-II band alignment have a much longer carrier lifetime. It is found that the carrier lifetime of InAs/$GaAs_{0.78}Sb_{0.22}$ QDs reaches 16.86 ns, which is about 8-times and 16-times longer than ones of InAs/$GaAs_{0.86}Sb_{0.14}$ QDs and InAs/$In_{0.18}Ga_{0.82}As$ QDs, respectively. The results obtained here show helpful for understanding of the band alignment and carrier recombination processes of InAs/GaAsSb QDs with different Sb components, and the potential to develop high conversion-efficiency IBSCs.

References

[1] Arsenijevic D and Bimberg D 2016 *Proc. SPIE* 9892, Semiconductor Lasers and Laser Dynamics VII, 98920S
[2] Arakawa Y and Sakaki H 1982 *Appl. Phys. Lett.* **40** 939
[3] Huang H, Duan J, Dong B, Norman J, Jung D, Bowers J E and Grillot F 2020 *APL Photonics* **5** 016103
[4] Golovynskyi S, Datsenko O I, Seravalli L, Trevisi G, Frigeri P, Gombia E, Babichuk I S, Lin D Y, Li B K and Qu J L 2020 *Semicond. Sci. Tech.* **35** 055029
[5] Guo D, Jiang Q, Tang M, Chen S, Mazur Y I, Maidaniuk Y, Benamara M, Semtsiv M P, Masselink W T, Salamo G J, Liu H and Wu J 2018 *Semicond. Sci. Tech.* **33** 094009
[6] Bimberg D 2018 *Nanophotonics* **7** 1245
[7] Yang X G, Wang K F, Gu Y X, Ni H Q, Wang X D, Yang T and Wang Z G 2013 *Sol. Energ. Mat. Sol. C* **113** 144
[8] Kim Y, Cho I W, Ryu M Y, Kim J O, Lee S J, Ban K Y and Honsberg C B 2017 *Appl. Phys. Lett.* **111** 073103
[9] Martí A, López N, Antolín E, Cánovas E, Luque A, Stanley C R, Farmer C D and Díaz P 2007 *Appl. Phys. Lett.* **90** 233510
[10] Liu H Y, Steer M J, Badcock T J, Mowbray D J, Skolnick M S, Navaretti P, Groom K M, Hopkinson M and Hogg R A 2005 *Appl. Phys. Lett.* **86** 143108
[11] Kim D Y, Hatch S, Wu J, Sablon K A, Lam P, Jurczak P, Tang M C, Gillin W P and Liu H Y 2018 *IEEE J. Photovolt.* **8** 741
[12] Liu W S, Wu H M, Tsao F H, Hsu T L and Chyi JI 2012 *Sol. Energ. Mat. Sol. C.* **105** 237
[13] Zhou C, Liang, B L, Liu J T, Wang Y, Guo Y N, Wang S F, Fu J S, Mazur Y I, Ware M E and Salamo G J 2019 *Opt. Mater.* **98** 109479
[14] Liu W S, Wang Y T, Qiu W Y and Fang C 2013 *Appl. Phys. Express* **6** 085001
[15] Chen T T, Cheng C L, Chen Y F, Chang F Y, Lin H H, Wu C T and Chen C H 2007 *Phys. Rev. B* **75** 033310
[16] Reyes D F, Ulloa J M, Guzman A, Hierro A, Sales D L, Beanland R, Sanchez A M and González D 2015 *Semicond. Sci. Tech.* **30** 114006
[17] Liao Y A, Hsu W T, Chiu P C, Chyi J I and Chang W H 2009 *Appl. Phys. Lett.* **94** 053101
[18] Hospodková A, Zíková M, Pangrác J, Oswald J, Kuldová K, Vyskočil J and Hulicius E 2013 *J. Cryst. Growth* **370** 303
[19] Jin C Y, Liu H Y, Zhang S Y, Jiang Q, Liew S L, Hopkinson M, Badcock T J, Nabavi E and Mowbray D J 2007 *Appl. Phys. Lett.* **91** 021102